Chang Yin-Cheng Chan, Uceu F. H. R. Suhuddin, Lars Rath, Felipe Labanca Bachiega, Benjamin Klusemann

Grain Structure Evolution Ahead of the Die During Friction Extrusion of AA2024

Document type
Conference paper | Author accepted manuscript / Postprint

This version is available at
https://doi.org/10.48548/pubdata-3837

Citation details
Chan, C. Y.-C., Suhuddin, U. F. H. R., Rath, L., Bachiega, F. L., & Klusemann, B. (2024). Grain Structure Evolution Ahead of the Die During Friction Extrusion of AA2024. In: Mocellin, K., Bouchard, PO., Bigot, R., Balan, T. (eds). Proceedings of the 14th International Conference on the Technology of Plasticity - Current Trends in the Technology of Plasticity. ICTP 2023. Springer, Cham, 422–428.
https://doi.org/10.1007/978-3-031-41341-4_43
First published: 29.08.2023

Grain structure evolution ahead of the die during friction extrusion of AA2024

Chang Yin-Cheng Chan[1][0000-0002-9684-4720], Uceu F.H. R. Suhuddin*[1][0000-0002-4000-4036], Lars Rath[1][0000-0002-7497-5201], Felipe Labanca Bachiega[1] and Benjamin Klusemann[1, 2][0000-0002-8516-5087]

[1] Solid State Materials Processing, Helmholtz-Zentrum Hereon, Geesthacht, Germany
[2] Institute for Production Technology and Systems, Leuphana University Lüneburg, Lüneburg, Germany
*`uceu.suhuddin@hereon.de`

Abstract. Friction extrusion (FE) is a thermo-mechanical process using a rotating die or feedstock to produce fully consolidated extrudates in different shapes, e.g. wires, rods and tubes. FE utilizes a non-consumable die to plastically deform material and generate heat by friction due to the relative rotation between the die and feedstock, i.e. FE represents a more energy-efficient process compared to classical extrusion techniques. In this study, the FE process is applied to extrude the Al-Cu alloy AA2024 using a 90 degree scroll-featured die. The grain structure evolution induced by thermo-mechanical processing is analyzed, in particular using the electron backscatter diffraction technique. Introduction of severe plastic deformation and high-temperature exposure induced by the die movement in radial and longitudinal directions relative to the materials enable grain refinement induced by dynamic recrystallization. The grain structure formation prior to deformation through the die orifice plays an essential role to obtain fully recrystallized homogeneous wires.

Keywords: Friction Extrusion, Grain refinement, Dynamic recrystallization.

1 Introduction

The friction extrusion (FE) process, developed and patented by Thomas et al. [1] in 1993, is an innovative forming technology that extrudes from solid billet, powder or chip materials. In FE, schematically shown in Fig. 1, the relative rotational motion between feedstock and non-consumable die imposes shear deformation, and the friction between them generates heat to plasticize material. The plasticized material is extruded into the die orifice, forming a fully consolidated extrudate in the shape of wire, rod or tube. No additional heat source is required, resulting in a distinct decrease in energy consumption [2]. Severe plastic deformation (SPD) coupled with high-temperature exposure initiates dynamic recrystallization (DRX), resulting in grain refinement within the extrudate. The grain refinement effect induced by SPD can generate even ultra-fine grained (UFG) structures in the submicron region and can achieve not only a strengthening effect but also innovative mechanical properties, such as superplasticity and high thermal stability [3, 4]. Therefore, UFG materials might be a suitable solution to deal with the typical strength-ductility trade-off dilemma.

In conventional extrusion, inappropriate processing parameters, such as temperature and extrusion rate, lead to defective and inhomogeneous microstructure, which also applies to the FE process. Consequently, extensive research on process parameters regarding defect-free and homogeneous extrudates has been conducted. Ansari et al. [5] and Baffari et al. [6] investigated the effect of rotational speed and extrusion force and determined the rotational speed as one decisive parameter in FE. Kalsar et al. [7] reported a homogeneous microstructure along the extruded wire manufactured by a scroll-featured 90 degree die angle and a reduction of the subsequent solution treatment time to reach the peak-aged T6 condition, compared to other extrusion techniques. Halak et al. [8] discovered two distinct extrusion modes by a lower die angle (60°), in which a fully recrystallized wire was successfully produced when sticking occurred at the die-feedstock interface. However, with processing time and temperature increase, the friction condition at the die-feedstock interfaces changed to sliding, resulting in an inhomogeneous microstructure within the wire. In contrast to the broad research on the properties of the extrudate, little literature addresses the phenomenon ahead of the die in FE. Li et al. [9] traced the material flow in the residual feedstock and derived the corresponding strain and strain rate ahead of the die. However, the grain structure homogeneity of the extrudate was not reported, which hinders the interpretation of the correlation between this finding and the extrudate microstructure. Wang et al. [10] disclosed the evolution of microstructure in homogeneous FE tubes in front of the die orifice and confirmed different types of DRX by correlating the distribution of high- and low-angle grain boundaries. Nonetheless, such investigation for a fully recrystallized wire is still missing.

To unveil the grain structure evolution induced by thermo-mechanical process in front of the die orifice for fully recrystallized wire, the present study analyzes the microstructure in the extruded wire as well as in the residual feedstock, in particular using the electron backscatter diffraction (EBSD) technique.

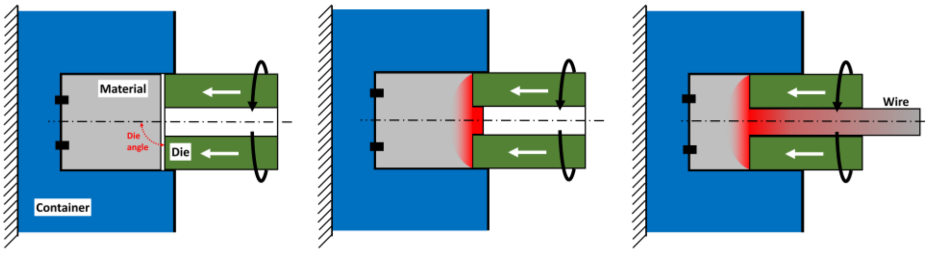

Fig. 1. Illustration of the FE process including relevant components.

2 Materials and Methods

AA2024 T351 billets were friction extruded by the dedicated friction extrusion machine FE100 manufactured by Bond Technologies. The container machined from 4140 steel with an inner diameter of 50 mm and an extrusion die with a 90 degree die angle from H13 steel machined with five spiral grooves with a 10 mm die orifice were deployed, which resulted in an extrusion ratio of 25. The beginning stage of the process utilized a rotational speed of 300 rpm with 50 kN to ensure complete contact between the extrusion die and feedstock. After the extrusion die advanced for 1 mm, a 10 s ramp stage to the velocity-controlled FE process was initialized. The constant rotating speed of 120 rpm and the two different extrusion rates of 10 and 4 mm/min represent the relevant process parameters in this study.

For microstructure analysis, longitudinal sections of the wires and the residual feedstock were prepared following standard metallography procedures and an electrolytic etching with Barker solution was applied for optical microscope (OM) observation using a Keyence VHX-6000 digital microscope and a Leica DMi8 OM. Additionally, the residual feedstock was subjected to a similar metallographic preparation followed by vibratory polishing with a colloidal silica solution for EBSD observations. The EBSD analysis was conducted using an FEI Quanta 650 field-emission scanning electron microscope (SEM) equipped with a Velocity EBSD system. Orientation mapping involving automatic beam scanning was performed with a scan step size of 0.2 µm. The obtained crystallographic data was expressed as EBSD maps in terms of inverse pole figure (IPF) mappings. A 15° criterion was applied to define low-angle grain boundaries (LAGBs) and high-angle grain boundaries (HAGBs).

3 Result and Discussion

To evaluate the microstructural homogeneity in the FE wires, three selected areas that are equally spaced along the radius of the wire longitudinal section for both extrusion rates were investigated and summarized in Fig. 2. Comparable fine-grained microstructures, with grain size below 10 µm, were observed in areas A and B for both extrusion rates. Larger grains are present at the periphery, which refer to the residual heat in the die bearing, boosting grain growth. In contrast, the grain structure at the center, area C in Fig. 2, shows a significant discrepancy. At the higher extrusion rate, elongated grains accompanying defects can be noticed. Two distinct elongated grain directions occurred, indicating unstable material flow and might explain the formation of defects at the boundary of incompatible material flow orientation. However, a homogeneously refined grain structure has been found in the 4 mm/min extrusion rate wire. A deeper investigation of the residual feedstock was conducted to understand the grain structure formation further.

Based on the grain morphology, the residual feedstock is divided into three regions, as shown in Fig. 3. Next to the base material (BM), the thermo-mechanically affected zone (TMAZ) is divided into two regions based on the different microstructures. The TMAZ 1 is adjacent to the die-feedstock interface and consists of a fine-grained structure, whereas in TMAZ 2, the elongated grains are dominating, describing the onset of mechanical effect imposed by the extrusion die. The outer region of the TMAZs pointed to the extrusion direction, indicating the inevitable extrusion happening due to the clearance between the extrusion die and the container wall. The TMAZ 1 in both processes share the approximately same shape with a major difference in the thickness at the center. At higher extrusion rate, the center of TMAZ 2 was extended to the extruded wire, indicating the origin of the elongated grain at the center and clarifying the variation of grain structure in the center of the wire extruded at different rates. The asymmetry observed in the wire extruded at higher extrusion rate further confirms the unstable material flow and the potential formation of defects. Although the shape of TMAZ 1 is similar in both processes, the volume in the low extrusion rate sample was considerably larger than in the high extrusion rate sample. The reason might refer to more heat accumulation and deformation due to a lower extrusion rate, resulting in a larger volume of softening material.

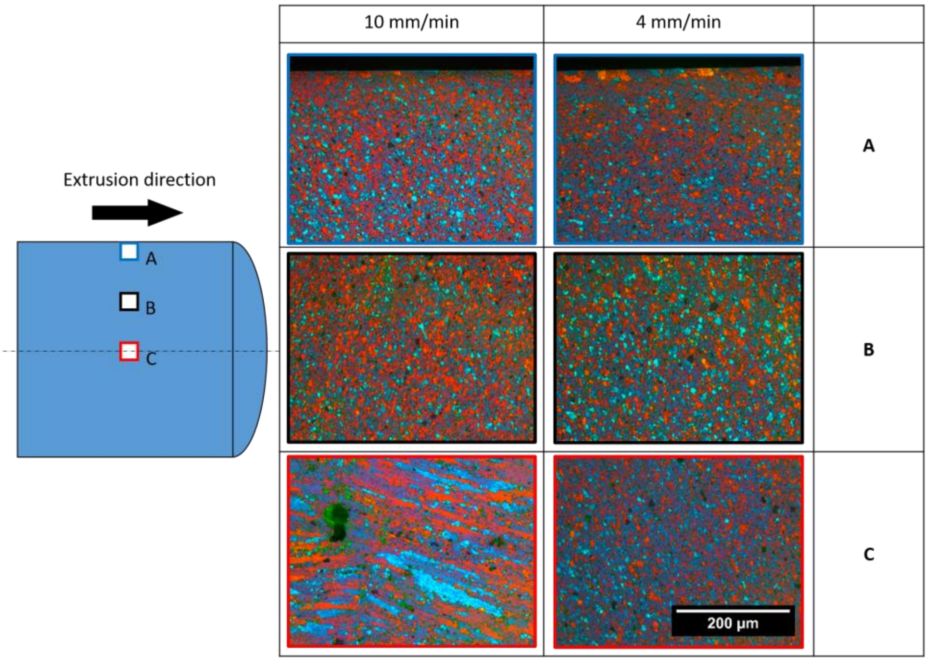

Fig. 2. OM micrographs of the wires at different positions within the wires, produced at two different extrusion rates.

The EBSD maps of BM, TMAZ 2 and TMAZ 1 in the residual feedstock at 4 mm/min extrusion rate are summarized in Fig. 4 a-c. A clear transition of grain structure from the elongated grain in BM to the fine-grained structure in front of the die can be observed. The typical elongated grain structure in the extruded BM, accompanied by large secondary phases at the grain boundaries, is presented in Fig. 4d. During FE, the large secondary phases were fragmented into fine secondary phases, as shown in TMAZ 1 in Fig. 4f. The grain size in the BM, which is represented by HAGB spacing in the vertical direction, is in average 14.1 µm. In the TMAZ 2, the elongated grains were fragmented and reoriented in a new direction, which differs from the original grain elongated direction as well as the extrusion direction, possibly due to the geometrical requirement of strain [11], resulting in the development of LAGBs within deformed grains and the decrease of the average HAGB spacing to 7.6 µm, as shown in Fig. 4b. Some of the LAGBs transformed into HAGBs as the misorientation angle exceeds 15°. As approaching the die-feedstock interface, the temperature and strain within TMAZ 1 increased, giving rise to the formation of a fine-grained structure with an average HAGB spacing of 4.6 µm, indicating further recrystallization, as presented in Fig. 4c. The formation of new grains induced by LAGB to HAGB transformation as a result of sub-grain rotation and thermal activation energy implies the occurrence of DRX, which can also been confirmed by the the equiaxed grain structure..

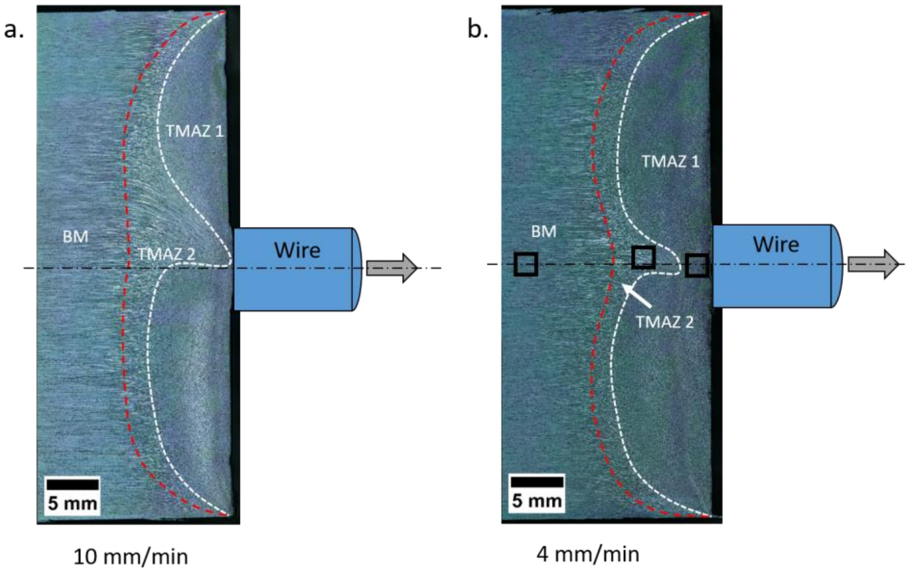

Fig. 3. Microstructure of residual feedstock at extrusion rates of (a) 10 mm/min and (b) 4 mm/min. The black rectangles are the position of conducting EBSD measurement, Fig. 4 b-c.

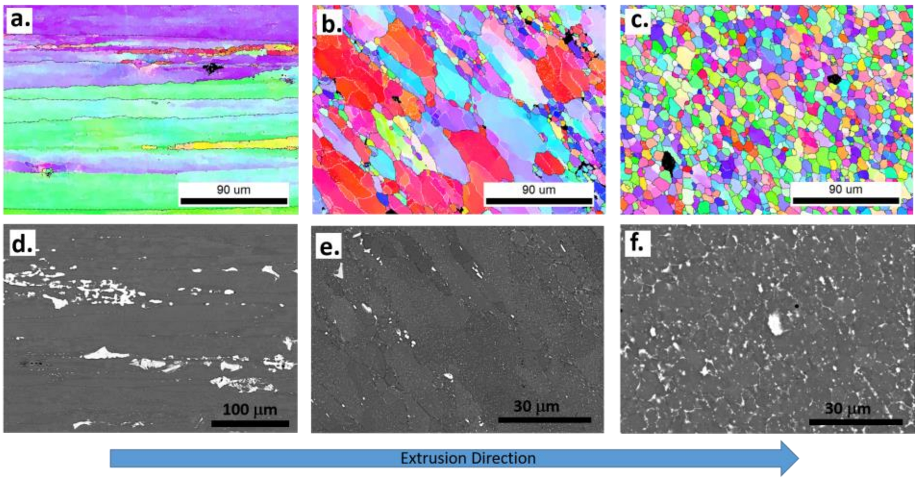

Fig. 4. Microstructure obtained from several regions in extrusion sample at 4 mm/min. The position within the residual feedstock are highlighted by rectangles in Fig. 3b: EBSD maps of BM (a), TMAZ 2 (b) and TMAZ 1 (c); SEM backscatter images of BM (d), TMAZ 2 (e) and TMAZ 1 (f).

4 Summary

In the present study, the grain structure formation in front of the extrusion orifice in friction extrusion and the homogeneity of the extruded wires were investigated. The fully recrystallized homogeneous wire was successfully extruded. The main findings are summarized as follows:

1. Fully recrystallized homogeneous wires were successfully extruded at 4 mm/min extrusion rate, due to a more stable material flow in front of the die.
2. Based on grain morphology, the microstructure in front of the die is divided into two thermo-mechanically affected zones (TMAZ), where TMAZ 1 comprises a recrystallized fine grain structure and TMAZ 2 consists of a deformed grain structure.
3. The elongated grains in the base material (BM) transformed into fully recrystallized grains in front of the die prior to entering the die orifice. Recrystallization induced by sub-grain formation, sub-grain rotation and thermal activation energy decreases HAGB spacing from 14.1 µm in BM to 4.6 in TMAZ 1.

Funding

This project has received funding from the European Research Council (ERC) under the European Union’s Horizon 2020 research and innovation programme (grant agreement No 101001567).

Data Availability

The data related to this research will be published under https://doi.org/10.5281/zenodo.7688908.

References

1. W.M. Thomas, E.D. Nicholas, S.B. Jones (1993) U.S. Patent 5,262,123.
2. D. Baffari, A.P. Reynolds, A. Masnata, L. Fratini, G. Ingarao (2019) Friction stir extrusion to recycle aluminum alloys scraps: Energy efficiency characterization. J. Manuf. Process. 43:63-69.
3. R. Lumley (2010) Fundamentals of aluminium metallurgy: production, processing and applications. Elsevier.
4. J.R. Croteau, J. Jung, S.A. Whalen, J. Darsell, A. Mello, D. Holstine, K. Lay, M. Hansen, D.C. Dunand, N.Q. Vo (2020) Ultrafine-grained Al-Mg-Zr alloy processed by shear-assisted extrusion with high thermal stability. Scr. Mater. 186:326-330.
5. M.A. Ansari, R.A. Behnagh, M. Narvan, E.S. Naeini, M.K.B. Givi, H. Ding (2016) Optimization of Friction Stir Extrusion (FSE) Parameters Through Taguchi Technique. Trans. Indian Inst. Met. 69:1351-1357.
6. D. Baffari, A.P. Reynolds, X. Li, L. Fratini (2018) Influence of processing parameters and initial temper on Friction Stir Extrusion of 2050 aluminum alloy. J. Mater. Eng. Perform. 28(1):4150-4161.
7. R. Kalsar, X. Ma, J. Darsell, D. Zhang, K. Kappagantula, D.R. Herling, V.V. Joshi (2022) Microstructure evolution, enhanced aging kinetics, and mechanical properties of AA7075 alloy after friction extrusion. Mater. Sci. Eng. A. 823:142575.
8. R.M. Halak, L. Rath, U.F.H.R. Suhuddin, J.F. dos Santos, B. Klusemann (2022) Changes in processing characteristics and microstructural evolution during friction extrusion of aluminum. Int. J. Mater. Form. 15(24).
9. X. Li, M. Reza-E-Rabby, A. Guzman, G. Grant, S. Mathaudhu, M. Hinton, A. Reynolds (2022) Strain and strain rate in friction extrusion. J. Mater. Res. Technol. 20:882-893.
10. T. Wang, J.E. Atehortua, M. Song, M. Reza-E-Rabby, B.S. Taysom, J. Silverstein, T. Roosendaal, D. Herling, S. Whalen (2022) Extrusion of Unhomogenized Castings of 7075 Aluminum via ShAPE. Mater. Des. 213:110374.
11. U.F.H.R. Suhuddin, S. Mironov, Y.S. Sato, H. Kokawa (2010) Grain structure and texture evolution during friction stir welding of thin 6016 aluminum alloy sheets. Mater. Sci. Eng. A. 527(7-8):1962-1969.